*Russian Geology and Geophysics* © 2019, V.S. Sobolev IGM, Siberian Branch of the RAS
*Vol. 60, No. 1, pp. 97–107, 2019* *DOI:10.15372/RGG2019007* *Geologiya i Geofizika*

# 3D Tomographic Inversion of TEM Sounding Data

**V.S. Mogilatov[a,b,] ✉, E.Yu. Antonov[a], A.N. Shein[a]**

[a]*A.A. Trofimuk Institute of Petroleum Geology and Geophysics, Siberian Branch of the Russian Academy of Sciences, pr. Akademika Koptyuga 3, Novosibirsk, 630090, Russia*
[b]*Novosibirsk State University, ul. Pirogova 2, Novosibirsk, 630090, Russia*

Received 15 June 2017; accepted 18 December 2017

**Abstract**—One of the main objectives of geoelectric prospecting is mapping of the consolidated low-conductivity basement geometry. To resolve the issue, it will be equally important to delineate local structures at the bottom of the sedimentary complex and to estimate the misinterpretation of results due to the presence of areas with nonuniform conductivity in the stratified geologic cross section. Another relevant objective of EM sounding is to resolve the problem of delineation of anticlinal oil and gas traps. The horizontally layered model with a local inclusion of 3D abnormal areas is certain to fit for the above-mentioned objectives. The study is concerned with the technique of nonstationary EM sounding. When applied for the solution of structural problems, this technique considers the uniform distribution of fields within relatively large volume units of the space explored. Consequently, it results in the more efficient application of the perturbation technique (Born approximation) for the solution of the forward electrodynamics problem. The study presents the findings of 3D tomographic inversion with the use of synthetic and physical modeling data. They definitely allow us to acknowledge that the proposed mathematical apparatus for 3D inversion based on Born linearization of the forward problem has proved to be quite applicable.

*Keywords:* transient electromagnetic (TEM) sounding, Born approximation, linearized inversion

## INTRODUCTION

Mapping of the consolidated low-conductivity basement geometry is considered to be one of the main geoelectric survey objectives. In this instance, the objective of local structures delineation at the bottom of the sedimentary complex and the task to estimate misinterpretation results will be both advantageous due to the presence of areas with nonuniform conductivity in the layered geological profile. The horizontally layered model with local inclusion of three-dimensional abnormal areas tends to fit for the above-mentioned objectives. Another important objective set by EM sounding will be the solution of the problem connected with delineation of anticlinal oil and gas traps. This problem also suggests the setting in the form of the combined one-dimensional model of a host medium and spatial inclusion with conductivity distribution which differs from the reference one.

Mathematical modeling of nonstationary fields in media with a composite geological structure appears to be a resource-consuming task although efficient finite difference algorithms and hybrid schemes are being applied. Approximated mathematical modeling plays an important role under such conditions. In most cases, physically adequate substitution of one model for another will considerably simplify modeling algorithms. In any case, the task of fast computation provision is still recognized to be the most-searched, because forward problems solution has proved to be a basis of the inverse geoelectrical problem-solving technique so far. Once based on the procedure of 3D forward problem solution for appropriately defined fitting of the parameterized three-dimensional heterogeneity, a common approach can hardly meet electrical surveyors' requirements because of the process slowness.

The technique of nonstationary EM sounding is discussed in this paper. This technique considers uniform distribution of fields within relatively large volume elements of the space explored. For this reason, the use of the perturbation technique and the Born approximation, in particular (Born, 1933) will be more efficient for the solution of the forward electrodynamics problem.

Perturbation techniques have found a use for computational modeling of electromagnetic fields in two- and three-dimensional media (Obukhov, 1967; Davydov, 1968; Kaufman and Tabarovsky, 1970a,b; Obukhov and Butkovskaya, 1974; Berdichevsky and Zhdanov, 1984; Tabarovsky et al., 1988; Epov and Antonov, 1999). Moreover, the Born approximation is widely applied for experimental data interpretation, that provides a linearization approach to the solution of inverse problems (Bleistein and Gray, 1985; Habashy et al., 1986; Oristaglio, 1989; Zhdanov, 2007). Further, the linearization approach to the solution of the 3D inverse problem could be implemented as part of a tomographic technology that is taken into consideration under study. The

✉Corresponding author.
*E-mail adress:* mvecs@yandex.ru (V.S. Mogilatov)

authors have proposed the approach of transient electromagnetic (TEM) sounding long ago (Mogilatov, 1999; Mogilatov et al., 1999; Mogilatov and Epov, 2000), but currently, we are able to demonstrate concrete research results.

## BORN APPROXIMATION

One of the most functional approaches to computational modeling of electromagnetic fields is based on linearization of integral equations, which appear to be a formal record of the exact solution. Forward problem linearization is accomplished by means of the perturbation theory apparatus. In this case, we limit ourselves to null and the first decomposition of original Fredholm integral equation of the second kind into Neumann series in the solution neighborhood for the one-dimensional reference medium. This approach is usually known as the Born approximation. Initially, the Born approximation was developed to describe mechanical photon dissipation (Born, 1933). Since that time, the concept of the technique has found a use for the development of approximated solutions in different fields of science. In particular, this technique is also applied to solve the problems of induction and electric logging, and TEM sounding, and others. Let's consider in brief this procedure.

Suppose that there exists a perturbation factor in relation to the base (reference) model in a certain medium volume $V$ $(\bar{x}, \bar{y}, \bar{z})$. We also admit that this perturbation factor depends linearly on the electric field, e.g., perturbation or disturbance of conductivity. The source having been cut off, Maxwell first equation will be as follows in this domain:

$$\operatorname{rot}\mathbf{H} = \sigma_0(z)\cdot\mathbf{E} + \Delta\sigma(x,y,z)\cdot\mathbf{E}. \quad (1)$$

On the condition that we represent the electromagnetic field in terms of superposition of normal ($\mathbf{E}^0$ and $\mathbf{H}^0$) and abnormal ($\mathbf{e}$ and $\mathbf{h}$) fields, and also admit that summand—$\Delta\sigma\cdot\mathbf{e}$ is smaller in comparison with other summands of the left-hand member of the first equation (1), we will get the equation system, where the first equation is:

$$\operatorname{rot}\mathbf{h} = \sigma_0\mathbf{e} + \Delta\sigma\mathbf{E}^0, \quad (2)$$

i.e., a one-dimensional problem with distributed extrinsic current is being considered. The solution of this problem is known and characterized by fast numeric implementation.

Let's develop such an algorithm for near-field TEM sounding. Thus, the source is a current loop with current—$I$, and radius—***a,*** and with a central point—$S = (x_0, y_0, z_0)$. In such a case, the electric field has the only component—$E_\varphi$ in the one-dimensional stratified medium, so the solution (until now in the frequency domain) will be as follows:

$$E^0_\varphi(x,y,z,S,\omega) = I\cdot e(x,y,z,S,\omega). \quad (3)$$

The perturbed area, which is taken in the form of a parallelepiped, could be represented by the sum total of electric dipoles with the moments: $dI = \Delta\sigma\cdot E^0_\varphi\cdot d\bar{x}d\bar{y}d\bar{z}$, where $E^0_\varphi$ is the normal (not disturbed) field, which is used as a substitute for the complete field. In such a case, we could also use the condition that the problem is symmetric in relation to current loop sources and a receiver. If we consider that perturbation $\Delta\sigma$ in the domain $V$ to have little effect on the TEM process, we'll obtain the solution of the one-dimensional problem (2) and, consequently, we will get 3D full-waveform data on the receiving loop with a central point—$R = (x, y, z)$, which will be represented as follows:

$$E(R,S,\omega) = E^0(R,S,\omega) + I\cdot\Delta\sigma\cdot\iiint_V e(\bar{x},\bar{y},\bar{z},S,\omega)e(\bar{x},\bar{y},\bar{z},R,\omega)\phi\,d\bar{x}d\bar{y}d\bar{z}. \quad (4)$$

Thus, equations (3) и (4) will be given adequate consideration. It is known that (for example (Mogilatov, 2014)):

$$E^0_\varphi(r,z,\omega) = -i\omega\mu\cdot I\cdot a\int_0^\infty J_1(\lambda r)J_1(\lambda a)\lambda X(\lambda,\omega,z)d\lambda, \quad (5)$$

where $J_1$ denotes the Bessel function, $r = \sqrt{(x-x_0)^2+(y-y_0)^2}$, *a,* the supply loop radius; *X,* the solution of one-dimensional problem in the spatial harmonics domain; $i = \sqrt{-1}$, the imaginary unit. Now the abnormal field, instead of (4), will be represented as follows:

$$\Delta E(R,S,\omega) = \Delta\sigma\cdot(i\omega\mu)^2 Iab\int_0^\infty\int_0^\infty T(\lambda,\lambda')\lambda\lambda' Z(\lambda,\lambda',\omega)d\lambda' d\lambda, \quad (6)$$

$$Z(\lambda,\lambda',\omega) = \int_{z_1}^{z_2} X(\lambda,\omega,\bar{z})X(\lambda',\omega,\bar{z})d\bar{z}$$

$$= \left[\frac{X'_z(\lambda)X(\lambda') - X(\lambda)X'_z(\lambda')}{\lambda^2-\lambda'^2}\right]\Bigg|_{z_1}^{z_2},$$

$$T(\lambda,\lambda') = J_1(\lambda a)J_1(\lambda' b)$$

$$\times\int_{x_1}^{x_2}\int_{y_1}^{y_2}\phi(S,R,\bar{x},\bar{y})J_1(\lambda r_1)J_1(\lambda' r_2)\,d\bar{x}d\bar{y},$$

$$r_1 = \sqrt{(\bar{x}-x_0)^2+(\bar{y}-y_0)^2},\ r_2 = \sqrt{(x-\bar{x})^2+(y-\bar{y})^2},$$

where $b$ is the receiving loop radius; $\{(x_j, y_j, z_j),\ j = 1, 2\}$ is the domain boundaries of the abnormal body (parallelepiped); $\phi$, the geometric factor taking into account mutual position of the source, the receiver and the body (angular coefficient). In this case, we used the properties of function ***X*** as the solution of the boundary value problem (Mogilatov, 2014). $Z$ should be also considered when $\lambda = \lambda'$.

The solution is viable in the time domain, in case IFT is applied the equations (4)–(6).

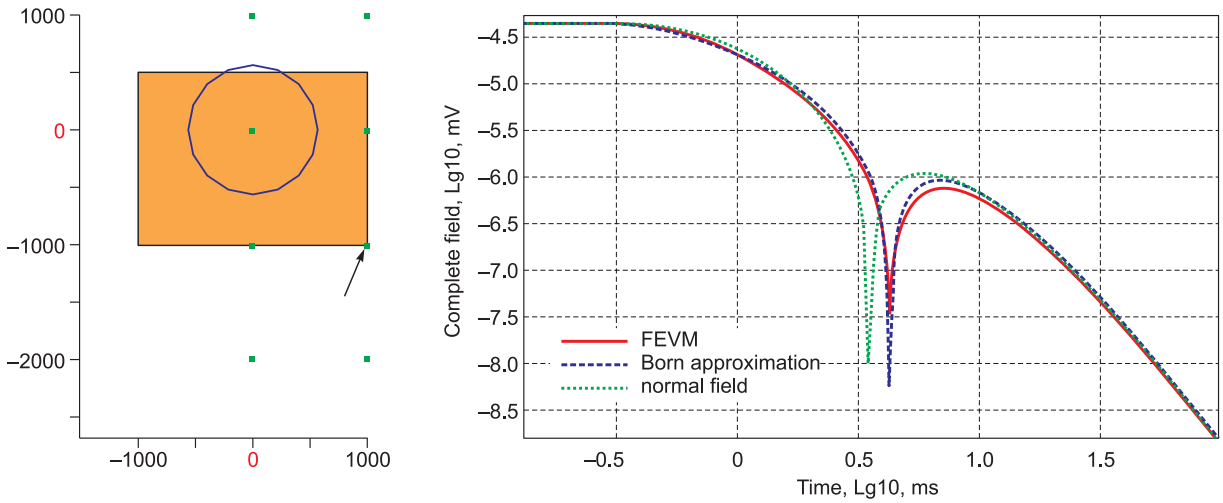


**Fig. 1.** The test model and comparison of FEVM and MAG3D calculation results. Normal and resultant fields.

$$F(x,y,z,t)=\frac{1}{2\pi}\int_{-\infty}^{\infty}\frac{1}{-i\omega}f(x,y,z,\omega)e^{-i\omega t}d\omega, \qquad (7)$$

where ω, the cyclic frequency; $t$, the time.

It should be noted that perturbation $\Delta\boldsymbol{\sigma}$ of the equations (4) or (6) could be left in the frequency domain or enclosed in the time domain. In the first case, it will be possible to use frequency-dependent disturbance (by the Cole–Cole formula), and therefore we will expand this solution on polarized 3D inclusion.

The MAG3D procedure, which allows implementation of the above-described algorithm, was tested by comparison with the exact calculation results obtained by the finite element vector method (FEVM) (Persova et al., 2010, 2011). Figure 1 presents the drawing and the log with regard to one of the applied models. The host medium is double-layered ($\rho_1$ = 100 Ohm·m, $h_1$ = 1000 m, $\rho_2$ = 1000 Ohm·m). The body along $X$ axis: from –1000 to 1000 m, along $Y$ axis: from –1000 to 500 m, along $Z$ axis: from –600 to –300m; ρ = 50 Ohm·m (conducting). The loop has the radius of 564 m, the central point (0, 1000 m), and current of 1 A.

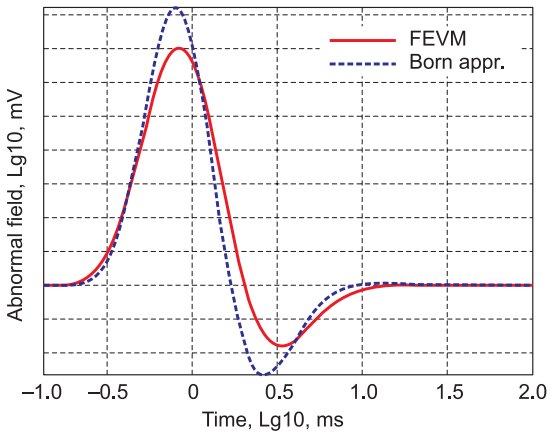


**Fig. 2.** Comparison of MAG3D and FEVM calculation results. Abnormal field.

Thus, we represent for comparison TEM curves ($dB_z/dt$) at the point of (1000, –1000) (indicated with an arrow in Fig. 1). The resultant fields calculated by FEVM and with the use of the Born approximation algorithm practically coincide with each other (Fig. 1). The result is obviously convincing. However, the TEM curve for the host medium (normal signal) is also shown in Fig. 1. It is seen that non-uniformity has a minor effect. For this reason, the Born approximation works quite well. Comparison of abnormal fields proves to be more illustrative. The comparison is presented in Fig. 2, and it serves as a confirmation of a satisfactory solution accuracy obtained by means of the Born approximation. With regard to the model given in Fig. 1, calculations carried out for other measuring points and for a different source position prove a good fit of the Born approximation with calculations done by FEVM. Anyway, it's not a simple answer to the question of how to estimate testing results of the program which uses intentionally approximated algorithm. We consider the obtained result to be highly satisfactory once the years of work experience acquired when dealing with synthetic and geoelectric survey field data are considered. The use of the linearized forward problem for the inverse problem solution will result in more objective estimation.

## TOMOGRAPHIC APPROACH TO TEM

The linear solution of the forward problem, which is offered in the equation (4), immediately implies the inverse problem solution with the use of linear inversion. Our approximation means the neglect of certain disturbances interaction between each other, but we are able to construct a linear system binding both field data and unknown particu-

lar perturbation within the range of the spatial elements of the explored medium domain. If we consider a distinctive approach to the medium description and the ways of inversion results representation, in principle, we will be able to make a claim for the tomography approach developed to solve the inverse problem. Although the tomographic approach is appreciated differently with regard to concrete EM techniques, it has been generally recognized in the field of stationary and quasi-stationary geoelectrical engineering, where a physical basement is characterized by Laplace and heat transfer equations. Certainly, we are far away from the fundamentals of classical X-ray tomography and even from seismic tomography equipped with ray-tracing and geometric optics.

Tomographic inversion is understood to be one of the ways of the inverse problem solution. There exists conventional wisdom, according to which tomographic inversion should provide fairly immediate results in the form of medium images (3D or cross-sections). It is achieved by applying common reductions or simplification. It is common practice for tomographic inversion to apply approximated and linearized solutions of the forward problem. This problem statement presupposes the use of an efficient linear inversion apparatus. Approximation (linearization) could be followed by simplification of the physical process model. Besides the forward problem quality, the following problems can arise: convenient parameterization of 3D medium structure as a set of standard internally uniform elements, linear inversion technique, and the problem of representation and inversion results estimation. All these problems could be reasonably resolved in the context of the tomographic approach, which main principles will be briefly formulated as follows:

(1) the perturbation area is created by a number of primitive elements;

(2) the linearized solution of a multidimensional direct problem is constructed in the neighborhood of a simple (one-dimensional or even nonuniform) reference model;

(3) inversion is based on reversal of the linear system, which correlates experimental data and perturbed geophysical parameters with regard to the reference medium;

(4) the medium structure is restored by the obtained spatial distribution of parameters (for example, electroconductivity).

The focal (but not equally significant for the whole approach) point of the proposed scheme appears to be an efficient solution of the forward problem via approximated linearized representation. The data set of experimental observations obtained under different conditions (registration time, position of sources and observation sites) must be correlated with corresponding approximated representations. In the result, we obtain the system of linear equations to determine the sum total of piecewise constant conductivity disturbances. It will be as follows:

$$\begin{aligned} E(t_1) &= E^0(t_1) + I_0 \cdot \sum_{j=1}^{K} \Delta\sigma_j \cdot G_j(t_1), \\ E(t_2) &= E^0(t_2) + I_0 \cdot \sum_{j=1}^{K} \Delta\sigma_j \cdot G_j(t_2), \\ &\cdots\cdots\cdots\cdots \\ E(t_i) &= E^0(t_i) + I_0 \cdot \sum_{j=1}^{K} \Delta\sigma_j \cdot G_j(t_i), \\ &\cdots\cdots\cdots\cdots \\ E(t_N) &= E^0(t_N) + I_0 \cdot \sum_{j=1}^{K} \Delta\sigma_j \cdot G_j(t_N), \end{aligned} \tag{8}$$

where $E^0$, denotes a transient signal of the host one-dimensional media; $K$, the number of standard solid elements (tomographic grid cells), into which the investigated medium portion was divided; $\Delta\sigma_j$, conductivity disturbance in the $j$th element relative to the host medium; $G_j(t_i)$, the linearized representation coefficients (defined above) of the forward problem; $N$, the number of measurements.

Having taken into consideration experimental data errors, we should use a considerable body of evidence, but not the greater number of unknowns. It is certainly supposed

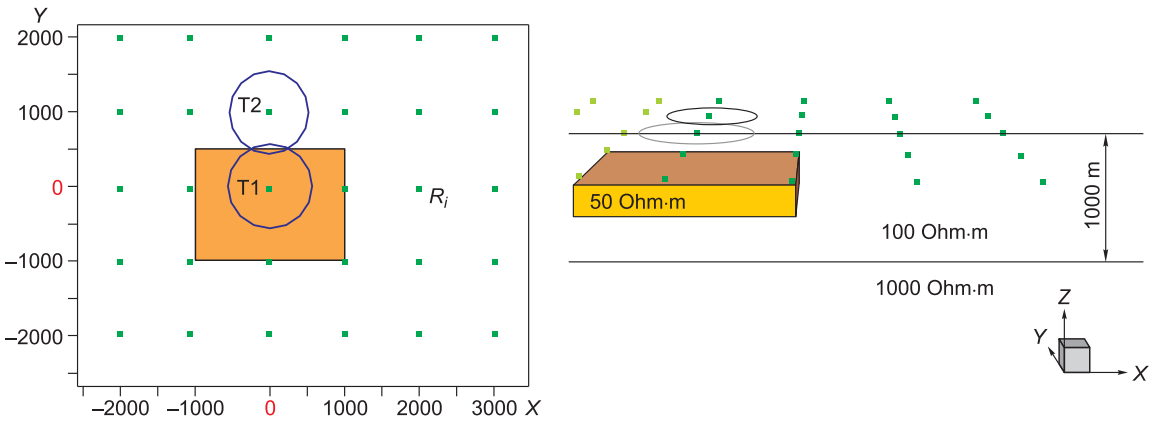


**Fig. 3.** The model. The layout and the profile.

that data (measurements) should be independent. Note that in case of transient signals use, each signal value determined at every time moment from each TEM curve will introduce its own equation into the system (8). Nevertheless, adjacent measurements on the TEM curve can hardly differ by informational value. In practice, it's easy to overdetermine the system (8) formally, but in reality, on physical grounds, it could be underdetermined. We are quite certain that the system (8) inversion reflects incorrectness of the inverse problem solution. It's highly unstable, ambiguous, and needs additional regularization.

Under such conditions we have to look for minimizing solution. A standard algorithm was used for the system inversion, it allows finding a common solution for the overdetermined system of equations, and it is based on the least-squares method and singular value decomposition (Wilkinson and Reinsch, 1971). In this case, the number of solutions is limited to the minimum norm that is in accordance with the real distribution of conductivity disturbance, which is more or less smooth. A user can choose a solution option depending on the number of used singular values.

## NUMERIC EXPERIMENTS DESCRIPTION

**Synthetic data.** We used the available three-dimensional calculations in accordance with the FE method carried out by M.G. Persova. The medium model is shown in Fig. 3, and the image is obtained with the use of GeoPrep software elements of graphic interface (M.G. Persova, Yu.G. Soloveichik).

Nonhomogeneity with the dimensions of 2000 × 1500 × 300 m and resistivity of 50 Ohm · m was placed into the double-layered geoelectric section. The top of nonhomogeneity is situated at a depth of 300 m. One can see that two positions of generator loops are used—T1 и T2 with a 564 m radius (in compliance with the 1000 × 1000 m square outline), and (0, 0) and (0, 1000) coordinates. The transient

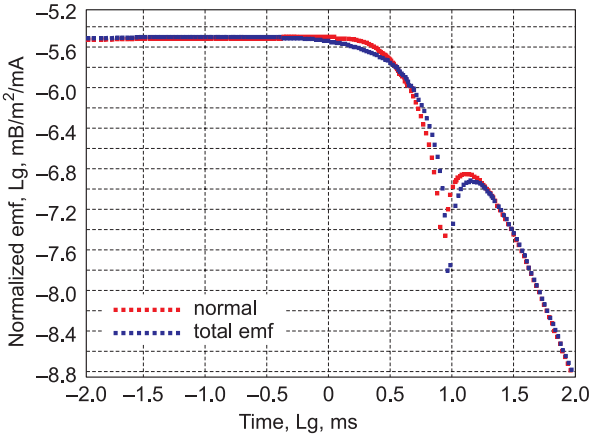


**Fig. 4.** The example of TEM curves.

process is registered from each of them at 35 points. In the result, we have the sum total of 70 TEM curves.

Figure 4 presents the example of TEM curves (normal and integral) at the point of X = 2000 m, Y = –1000 m. These are mathematical curves, which are "long" (166 time moments) with redundant inception and late stages, at which the nonuniformity effect is missing. The experimental setting drawbacks are thought to be rather a small difference between the two source positions and the presence of large spans (>4 km), where the signal and the body influence in particular are weak. We have left it still unchanged. Based on correlation results for the host medium and integral curves, we came to the conclusion that the anomalous effect is little and tends to be localized in the time domain where the curves alternate in signs, that is in the neighborhood of signal zero values. This fact implies difficulties of conventional approaches application with the use of apparent values.

**The first stage.** The experiment yielded 70 TEM curves from two generator loops. The nonhomogeneity position (even its presence) is considered to be unknown at the first

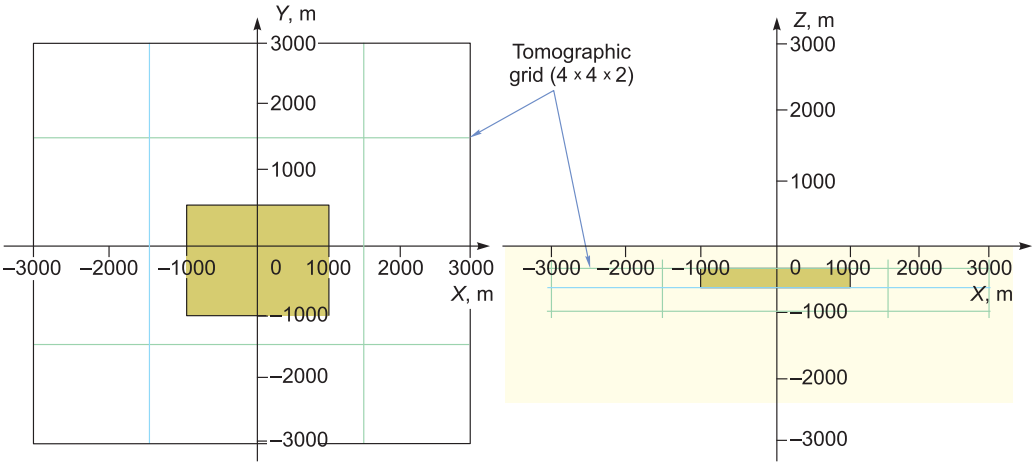


**Fig. 5.** The coarse tomographic grid.

| Y/X(m) | –2250 | –750 | 750 | 2250 |
|---|---|---|---|---|
| Layer 1 | | | | |
| 2250 | 0.100E+03 | 0.111E+03 | 0.111E+03 | 0.111E+03 |
| 750 | 0.999E+02 | 0.892E+02 | 0.892E+02 | 0.999E+02 |
| -750 | 0.999E+02 | 0.468E+02 | 0.468E+02 | 0.999E+02 |
| –2250 | 0.100E+03 | 0.998E+02 | 0.998E+02 | 0.100E+03 |
| Layer 2 | | | | |
| 2250 | 0.100E+03 | 0.100E+03 | 0.100E+03 | 0.100E+03 |
| 750 | 0.100E+02 | 0.100E+02 | 0.100E+02 | 0.100E+02 |
| -750 | 0.999E+02 | 0.984E+02 | 0.968E+02 | 0.999E+02 |
| –2250 | 0.100E+03 | 0.999E+02 | 0.999E+02 | 0.100E+03 |

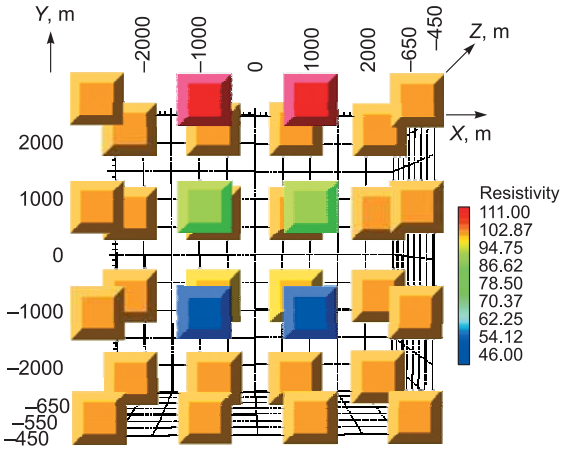


**Fig. 6.** The inversion result on the coarse tomographic grid.

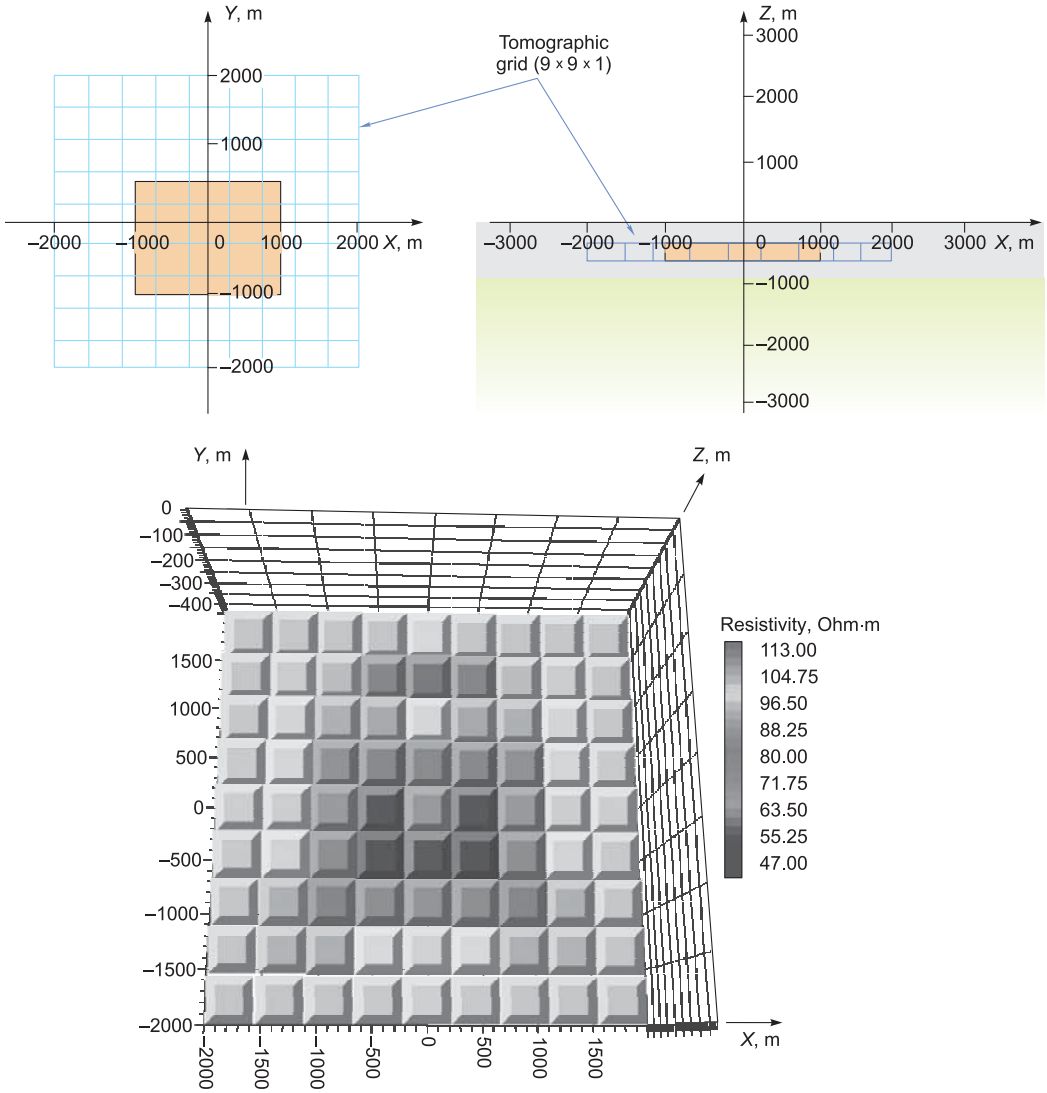


**Fig. 7.** The expanded tomographic grid.

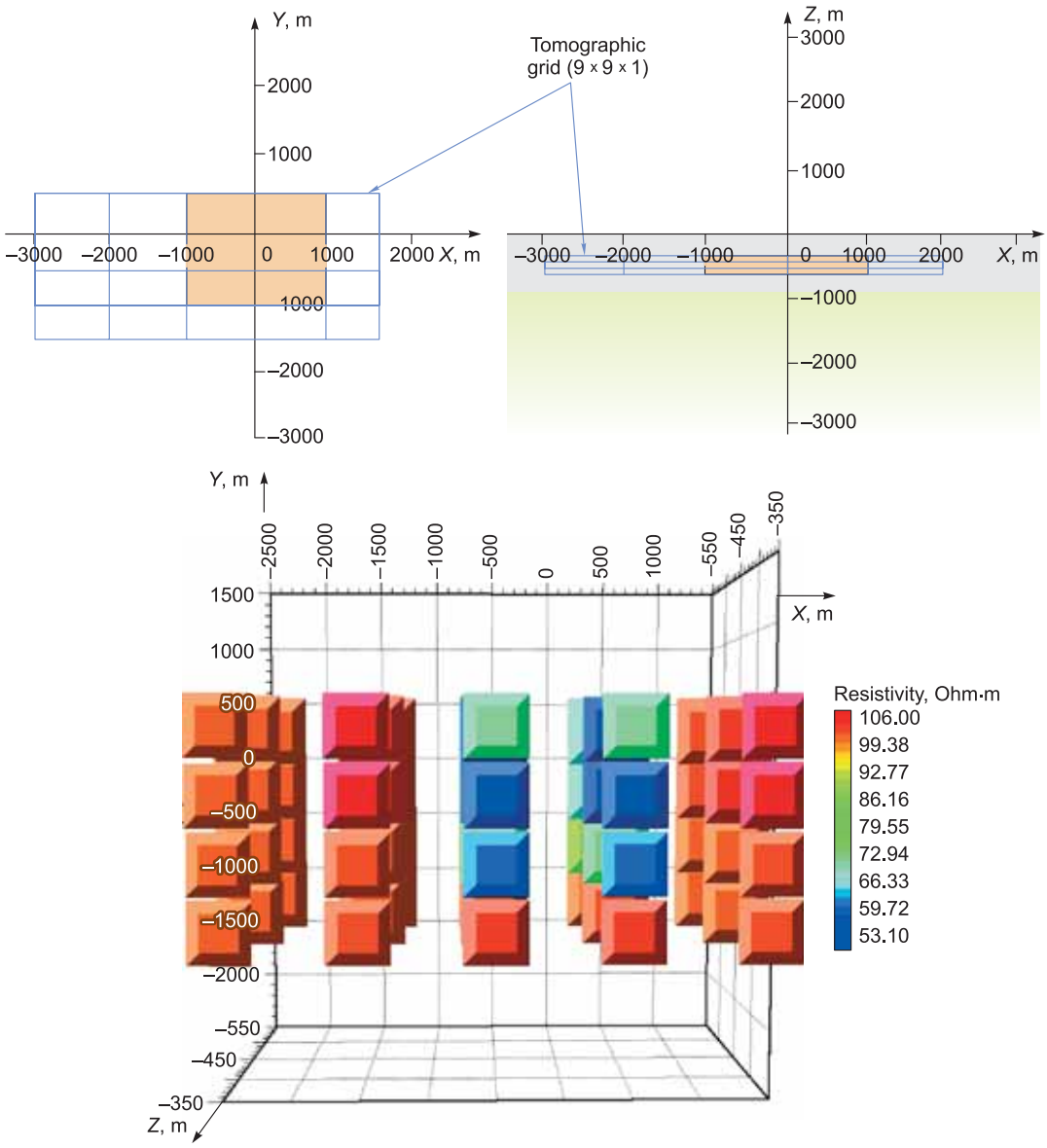


**Fig. 8.** Another example of tomographic inversion. The model, the grid and the result.

stage of the experiment. In this case, we suppose that the area of sounding tends to be too large—3000 × 3000 m. Firstly, we will take a closer look at the 4 × 4 × 2 km 3D tomographic grid, which is shown in Fig. 5. Two deep layers ($-1000 < z < -600$ and $-600 < z < -300$ (measured in meters)) are investigated. Then, we will determine conductivity disturbances for the known host medium in 32 cells of the tomographic grid.

According to the above-given description, tomographic inversion implies the fulfillment of the definite procedures, where the first one (grid generation) has been implemented. Now with regard to the chosen grid, we should do coefficients calculations for each element, i.e., to construct a linearized solution for the 3D forward problem. Further, the parameters of the host cross-section ought to be determined (e.g., through preliminary one-dimensional interpretation). Coefficients calculations (in accordance with equations (4)–(8)) turn out to be the most resource-intensive part of the proposed mathematical apparatus. We have to compute and store the definable functions—coefficients in the amount of— $N_x \times N_y \times N_z \times N_t$, where $N_x$, the number of the grid partitions along $X$ axis; $N_y$, the number of the grid partitions along $Y$ axis; $N_z$, the number of the grid partitions along $Z$ axis; $N_t$, the number of TEM curves invoked from all the generators and receivers being multiplied by the number of timing cycles or tick marks. In this case, we will obtain $4 \times 4 \times 2 \times 70 = 2240$ functions—coefficients, each of them is determined for 166 timing cycles.

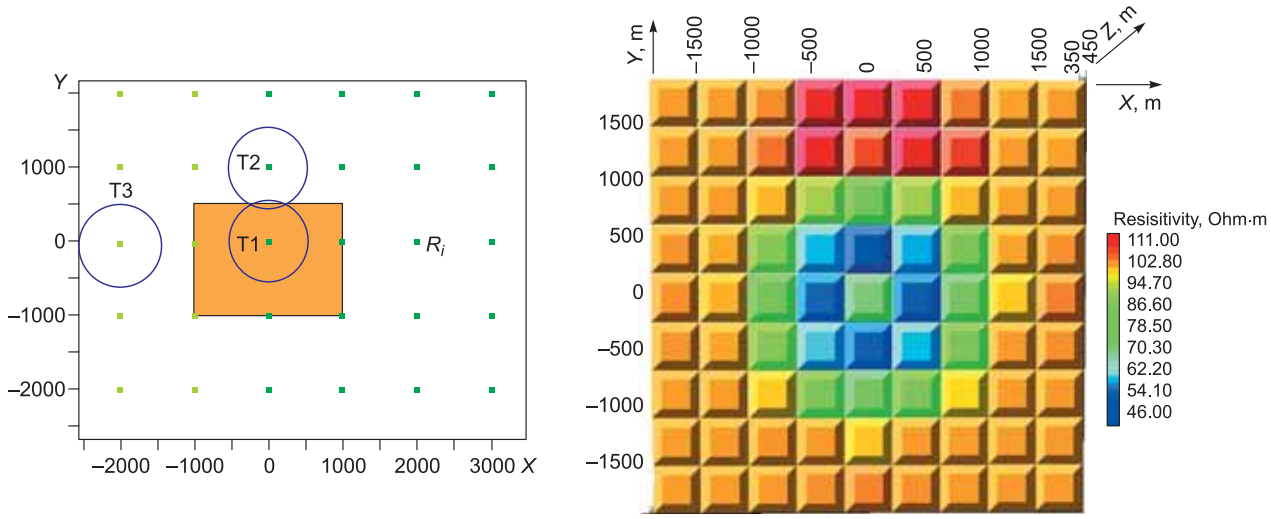


**Fig. 9.** The model. The layout and the profile.

Therefore, the linear system from 70 × 166 (in our case) equations is developed, where the right part is the difference between pseudo-experimental and estimated data for the normal medium. The system coefficients are once calculated and saved; and $N_x \times N_y \times N_z$ unknowns appear to be conductivity disturbances ($\Delta\sigma$) in each primitive medium partition element.

Linear system solution is carried out by the least-squares method and regularization (the least norm). This is a fast procedure (using preliminary calculated coefficients calculations) because it can be repeated through altering inversion parameters (if it is necessary) and/or predetermining certain elements as known variables (e.g., relief attributes and upper part of the profile).

Figure 6 presents layer-by-layer results of tomographic inversion. *X* and *Y* coordinates are placed in the cell centers of the tomographic grid in the table of Fig. 6.

The figure shows that four elements (cells) of the upper layer ($-600 < z < -300$) are apparently distinguished by resistivity, and in the table they are color-coded. Here the result is presented in a 3D graphical format. It should be noted that ways and means of visual representation of inversion results prove to be the essential part of the tomographic approach.

**The second stage, the expanded grid.** The first inversion stage enabled us to carry out rough localization of the abnormal body, that's why at the second stage we can generate more expanded grid in the domain of smaller dimensions (Fig. 7). One layer has been studied in vertical direc-

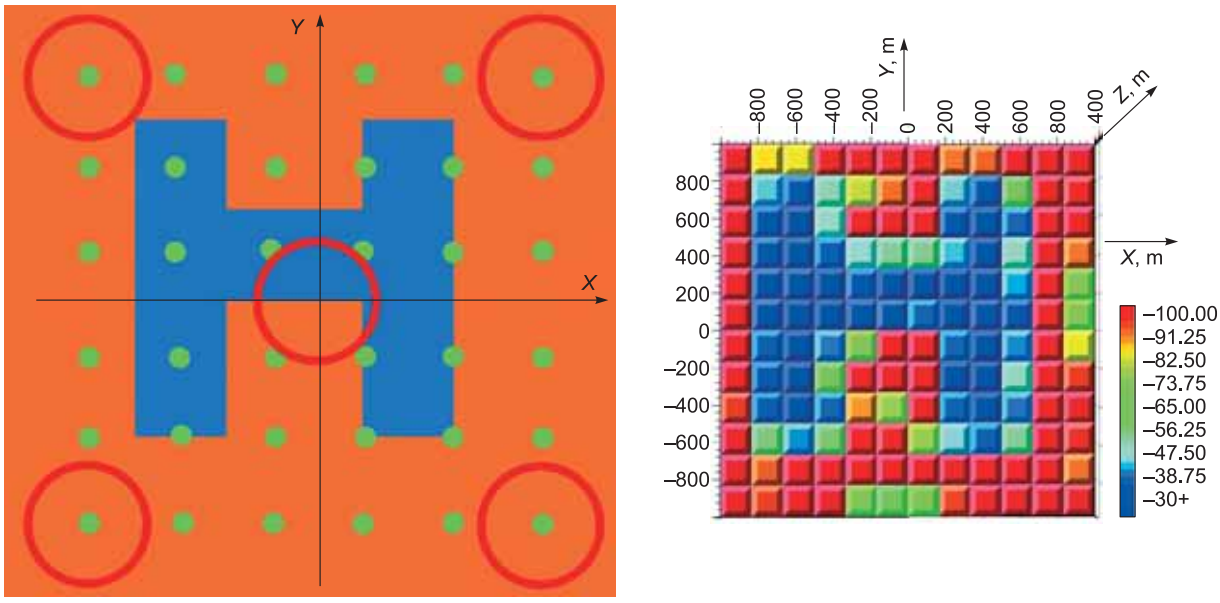


**Fig. 10.** Multiple nonhomogeneity. The inversion of transient signals from the generator loop central position.

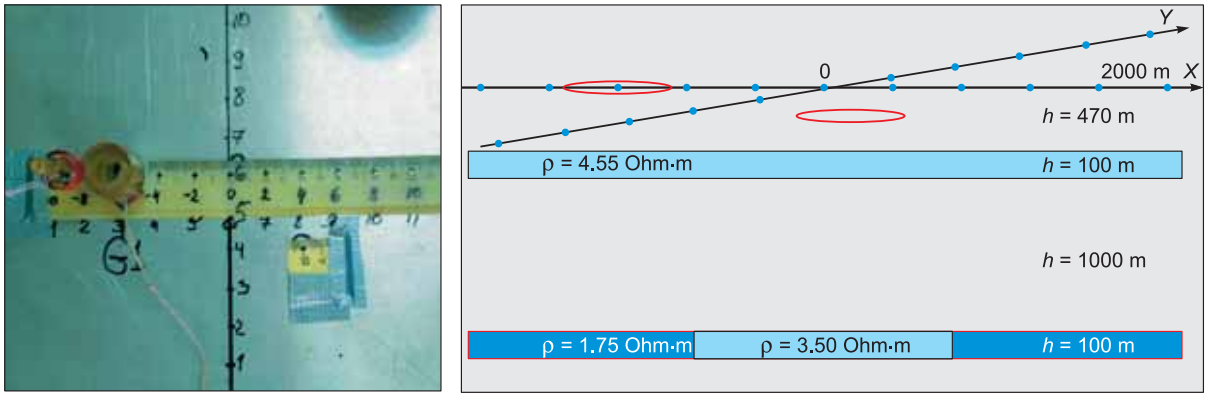


**Fig. 11.** Physical modeling**.** The photo of the experimental set-up (on the left) and the observation system.

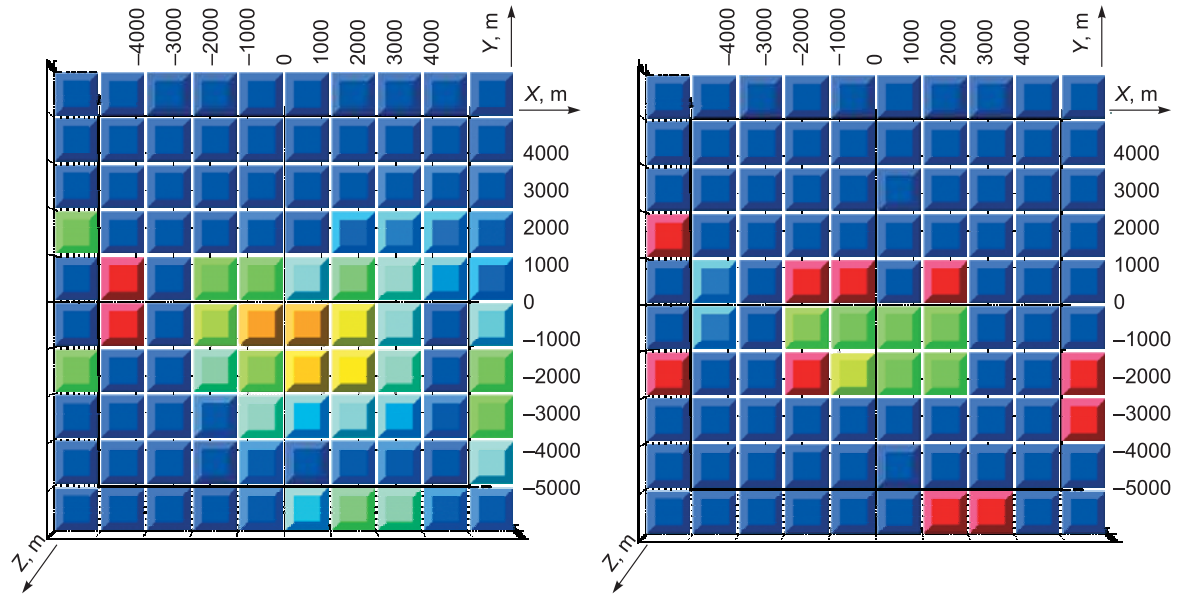


**Fig. 12.** Inversion results for different parameters of regularization.

tion; the result of tomographic inversion is represented in a graphical format in Fig. 7.

The figure illustrates that the position, the shape of the nonhomogeneity and its resistivity have been defined with rather high accuracy. The process of abnormal body specification could be continued. However, the findings are limited both to linear approximation accuracy and the accuracy of a priori information about the host medium, and to the quantity and quality of field data.

**More inversion examples.** Let's consider one more example of tomographic inversion for the same model and the same "field" data. Here we will conduct extensive investigation of the target horizon in three layers (100, 100, and 100 m) (Fig. 8).

Up to now we have applied synthetic data supplied by M.G. Persova. It was of great interest to deal with calculations of another 3D modulation program. We used Modem3D program (application designers M.I. Ivanov, I.A. Kremer, and V.A. Kateshov), where the finite elements vector method (FEVM) was also implemented (Ivanov et al., 2007, 2009; Shein et al., 2012; Shein, 2013; Shein et al., 2014, 2015). To establish control, the same model and the set of receivers were used, but the observation system was fitted with the third source (Fig. 9).

**Complex arrangement/inclusion.** Another efficient result should be given consideration, when the loop with complex nonuniformity (Fig. 10) is being recovered according to area registration of a transient signal from fixed sources. The host medium is the same as in the previous examples (1000 m layer, 100 Ohm · m resistivity on the basement with resistivity of 1000 Ohm · m). Nonhomogeneity covers vertically the range from 300 m to 600 m, resistivity amounts to 30 Ohm · m. Five generator loops were used; the response was registered in 36 points of the survey grid with the interval of 400 m (Fig. 10).

Particular emphasis should be placed on the special feature of this numerical experiment. We managed to obtain synthetic data by means of linearized representation of the forward problem (the forward problem involves Born approximation). Thus, it could be only "internal" validation of the inversion algorithm by status. However, we introduced disturbances in the form of misalignment of the tomographic grid (12 × 12) lines with the nonhomogeneity borders. In such a way, quite a new result for methodological guidelines was received. It was found out that the inversion with five generator loops (in this case, only 9 observation points were exploited, so there were 45 curves in all) doesn't improve the inversion with the use of signals from one central source. The fact is that the adverse impact will rise with the distance increase, but data received in the vicinity of generator loops tend to suppress this abnormal effect.

**Physical modeling.** Finally, attention should be drawn to the result, which is certain to be a step forward to tomographic inversion of real field data. A.K. Zakharkin, a famous expert in physical modeling, has modeled TEM processes on sheets of metal at our request. Then the data and the model were recalculated with provision for electrodynamic similarity on full scale. The model is shown in Fig. 11, which also gives an overview of the observation system which is made up of responses at 22 points from one of the two generator loops: there are 44 TEM curves in all. Tzikl-7 standard equipment is used for registration. The section consists of two conductive beds, and there is an insert (5.5 × 5.5 km) of low conductivity in the bottom layer (evenly drilled holes in the sheet of metal).

The results shown in Fig. 12 indicate the capability to restore position, dimensions and even shape. It should be recognized that modeling was not superior in quality. The host medium was not consistent (owing to the bending of metal strata). Generally speaking, measurement errors definitely simulated acquisition conditions.

## CONCLUSIONS

The study of the 3D tomographic inversion procedure with the use of physical and mathematical modeling data allows us to conclude that the proposed mathematical apparatus for 3D inversion based on the Born linearization of the forward problem has proved to be quite applicable. It may be said that we are ready to initiate the next step, i.e., field data application. The tomographic approach should incorporate utility software for real-time visual interaction with database and graphic tools for results representation. It is beyond argument that a correct solution procedure of 3D forward problem will ensure fast tomographic inversion. The study results were obtained with the involvement of accurate 3D modeling, so we express particular gratitude to the application designers M.G. Persova, M.I. Ivanov, and I.A. Kremer. The data of physical modeling obtained by A.K. Zakharkin were of great practical value.

## REFERENCES

Berdichevsky, M.N., Zhdanov, M.S., 1984. Advanced Theory of Deep Geomagnetic Sounding. Elsevier Science Publ. Co., Inc.

Bleistein, N., Gray, S.H., 1985. Extension of Born inversion method to the depth dependent reference profile. Geophys. Prosp. 33 (7), 999–1022.

Born, M., 1933. Optik. Springer, Berlin.

Davydov, V.M., 1968. Random source electromagnetic field above gently-sloping structures. Geologiya i Geofizika, № 6, 83–91.

Epov, M.I., Antonov, E.Yu., 1999. Direct problems of electromagnetic sounding with account of geoelectric parameters dispersion. Fizika Zemli, No. 3–4, A48–A55.

Habashy, T.M., Chew, W.C., Chow, E.Y., 1986. Simultaneous reconstruction of permittivity and conductivity profiles in a radially inhomogeneous slab. Radio Sci. 21 (4), 635–645.

Ivanov, M.I., Kateshov, V.A., Kremer, I.A., Urev, M.D., 2007. Solution of 3D nonstationary problems of pulse geoelectric survey. Avtometriya 43 (2), 33.

Ivanov, M.I., Kateshov, V.A., Kremer, I.A., Epov, M.I., 2009. Modem 3D software for nonstationary sounding data interpretation with account of effects caused by polarization. Zapiski Gornogo Instituta 183, 242–245.

Kaufman, A.A., Tabarovsky, L.A., 1970a. Electromagnetic field above gently-sloping structures (two-dimensional problem), in: Electromagnetic Fields in Geophysical Prospecting Methods [in Russian]. Novosibirsk, Vol. 54, pp. 5–31.

Kaufman, A.A., Tabarovsky, L.A., 1970b. The Fundamentals of MT Sounding in the Low-Angle Structures Media [in Russian]. Nauka, Novosibirsk.

Mogilatov, V.S., 1999. Secondary sources and linearization in geoelectric problems. Geologiya i Geofizika (Russian Geology and Geophysics) 40 (7), 1102–1108 (1087–1094).

Mogilatov, V.S., 2014. Pulse Geoelectrical Engineering [in Russian]. Novosibirsk. Gos. Univ., Novosibirsk.

Mogilatov, V.S., Epov, M.I., 2000. Tomographic approach to interpretation of geo-EM sounding data. Fizika Zemli, No. 1, 78–86.

Mogilatov, V.S., Epov, M.I., Isaev, I.O., 1999. Tomographic inversion of TEM data. Geologiya i Geofizika (Russian Geology and Geophysics) 40 (4), 637–644 (621–628).

Obukhov, G.G., 1967. Horizontal electric dipole field above small irregularities of an insulating basement. Prikladnaya Geofizika 50, 124–131.

Obukhov, G.G., Butkovskaya, A.I., 1974. Application of TEM technique in the near-field zone and in a horizontally nonhomogeneous medium. Prikladnaya Geofizika 73, 132–143.

Oristaglio, M.L., 1989. An inverse-scattering formula that uses all the data. Inverse Problems 5 (6), 1097–1105.

Persova, M.G., Soloveichik, Yu.G., Domnikov, P.A., Simoe, E.I., 2010. The tomographic approach to interpretation of EM sounding data in three-dimensional media, in: Proc. 10th Int. Conf. "Main Issues of Electronic Instrument Engineering", FPEP–2010 [in Russian]. NSTU, Novosibirsk, Vol. 6, pp.150–155.

Persova, M.G., Soloveichik, Yu.G., Trigubovich, G.M., 2011. Computer modeling of geoelectromagnetic fields in three-dimensional media by the finite element method. Izvestiya, Physics of the Solid Earth 47 (2), 79–89.

Shein, A.N., 2013. The specific features of Modem 3D program applied for computing of non-stationary electromagnetic fields in 3D media, in: Proc. All-Russian Sci. Conf., Vol. 2 [in Russian]. Kirilitsa, Staryi Oskol, pp. 99–104.

Shein, A.N., Antonov, E.Yu., Kremer, I.A., Ivanov, M.I., 2012. TEM data Interpretation by the Modem 3D program for 3D modeling of transient electromagnetic field, in: Proc. 6th Int. Siberian Early Career GeoScientists Conf. (9–23 June 2012, Novosibirsk) [in Russian]. Novosibirsk. Gos. Univ., Novosibirsk, pp. 303–304.

Shein, A.N., Mogilatov, V.S., Antonov, E.Yu., 2014. Testing of 3D tomographic inversion of TEM sounding data with the use of linear (Born) approximation, in: Proc. 10th Int. Sci. Conf. "Natural Resources Management. Mining. Trends and Techniques in Prospecting, Survey, and Mining", Interecspo GEO-Siberia (8–18 April, 2014, Novosibirsk), Vol. 3 [in Russian]. SGGA, Novosibirsk, pp. 159–164.

Shein, A.N., Mogilatov, V.S., Antonov, E.Yu., 2015. The limits of tomographic approach to 3D inversion of TEM sounding data with the use of linear (Born) approximation, in: Proc. Int. Sci. Conf. "Natural Resources Management. Mining. Trends and Techniques in Prospecting, Survey, and Mining. Geo-Ecology", Interecspo GEO-Siberia. Geoecologiya 2 (2), 294–298.

Tabarovsky, L.A., Epov, M.I., Antonov, E.Yu., 1988. EM Field in the Media with Weakly Nonhorizontal Boundaries [in Russian]. IG&G, Novosibirsk (Available from VINITI 04.08.88, No. 6258-B88).

Wilkinson, J.H., Reinsch, C., 1971. Handbook for Automatic Computation. Vol. 2: Linear Algebra. Springer-Verlag, Berlin.

Zhdanov, M.C., 2007. The Theory of Inverse Problems and Regularization in Geophysics [in Russian]. Nauchnyi Mir, Moscow.

*Editorial responsibility:* M.I. Epov